Shape Change as an Indicator of Mechanism in the High-Pressure Structural Transformations of CdSe Nanocrystals

Juanita N. Wickham, Amy B. Herhold,* and A. P. Alivisatos
Department of Chemistry, University of California, Berkeley, California 94720
(Received 15 July 1999)

X-ray diffraction was used to monitor the structure of 45 Å diameter CdSe nanocrystals as they transformed repeatedly between fourfold and sixfold coordinated crystal structures. Simulations of the diffraction patterns reveal that a shape change occurs as the crystals transform. They also show that stacking faults are generated in the transition from the high- to the low-pressure phase. The shape change and stacking fault generation place significant constraints on the possible microscopic mechanism of the phase transition.

PACS numbers: 62.50.+p, 61.46.+w, 64.70.Kb, 68.35.Rh

The preparation of solids with novel bonding geometries is limited by our incomplete understanding of metastability. Theory can accurately predict the ground state structure of a solid for a given composition [1], but cannot accurately estimate the lifetime of a metastable state [2]. Accurate estimates of the metastability of different bonding geometries requires a clear understanding of the microscopic mechanisms by which solids transform between crystal structures. The study of solid-solid phase transitions in nanocrystals can potentially be very helpful in developing such microscopic pictures.

The importance of nanocrystals to the study of solid-solid phase transitions can be understood by analogy to magnetization reversal. A nanometer-sized magnetic crystal acts as a single magnetic domain, and simple models show that the time required for this domain to reverse its magnetic orientation is exponentially dependent upon the nanocrystal volume [3]. Sufficiently large magnetic crystals display qualitatively different kinetic behavior because they contain equilibrium defects and domain walls, which substantially lower the barriers to reversal [4]. Nanocrystals can also be viewed as "single structural domains." Studies of the kinetics of solid-solid phase transitions in nanocrystals [5] bear a striking resemblance to the analogous studies of magnetization reversal, with single nucleation events per nanocrystal [6], and with relaxation times strongly increasing in larger sizes [7,8].

There is, however, a key difference between the magnetic and the structural phase transitions in nanocrystals. As we have shown previously for solid-solid phase transitions in Si [9], nanocrystals change shape during structural transformations. Here we show that a systematic study of the shape changes through multiple transformation cycles can place strong constraints on the microscopic motions connecting the two phases. The present study focuses on fourfold to sixfold coordinated transformations in the prototypical colloidal semiconductor nanocrystal system, CdSe. Shape changes determined by diffraction simulations show that the mechanism of transformation is different for CdSe from that of Si, and also from previously proposed mechanisms for CdSe itself.

CdSe crystallites with an average size of 45 Å (standard deviation in size of $\sim 6\%$) were synthesized by literature methods [10]. The crystallites were passivated by a monolayer of trioctylphosphine oxide and soluble in a variety of organic solvents. Nanocrystals dissolved in the pressure-transmitting medium, ethylcyclohexane, were loaded into a Merrill-Bassett diamond anvil cell with a diffraction slit. X-ray diffraction patterns were collected on wiggler beam-line 10-2 at the Stanford Synchrotron Radiation Laboratory with 12.5-keV x rays. Patterns were collected with image plates for 12 minutes in an angle-dispersive geometry, with an instrument resolution of $0.01Q(\text{Å}^{-1})$. The pressure was changed in 0.5–1 GPa steps that were spaced by approximately 1 hour, and measured using standard ruby fluorescence techniques [11].

Volume versus pressure curves for two complete cycles of the phase transition (same sample) are shown in Fig. 1. The experiment clearly shows massive hysteresis as compared to the bulk [12], behavior that is characteristic of defect-free nanocrystals and consistent with previous high-pressure studies of CdSe nanocrystals [13]. [Stacking faults, which are present in the nanocrystals according to transmission electron microscopy (TEM) and x-ray diffraction (XRD) measurements, have little influence upon the phase transition pressure and kinetics, a fact that will be discussed in detail below.] The two consecutive cycles overlap within experimental error, implying that no new high-energy defects are created during the nanocrystal transformation, which is also markedly different from what is observed in the bulk [14]. Representative x-ray diffraction patterns from each cycle are presented in Fig. 2 (black).

Previous work on the shape change of Si nanocrystals [9] utilized the widths of specific peaks to elucidate shape changes. However, the nanocrystals discussed here are much smaller (45 Å instead of 500 Å in diameter), so that not just linewidths but line shapes and relative

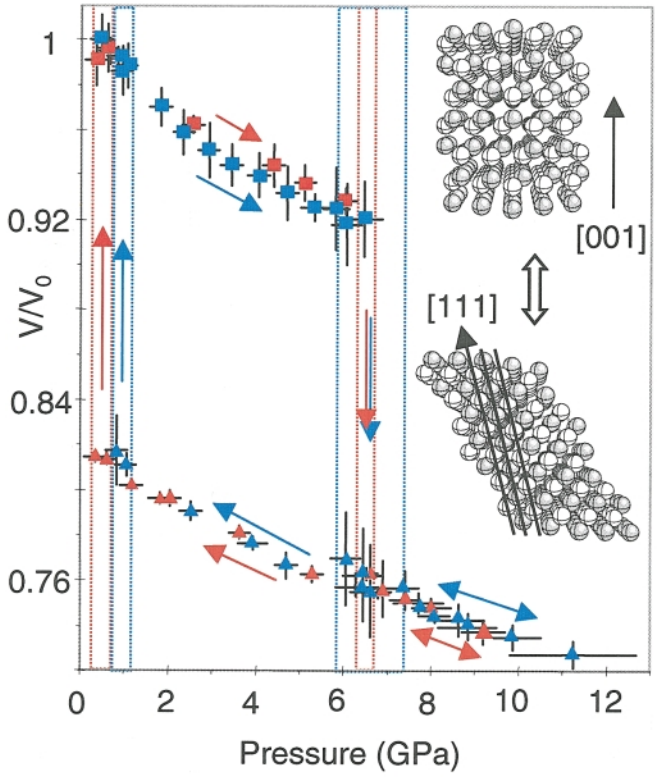

FIG. 1 (color). Multiple hysteresis cycles of 45 Å CdSe nanocrystals showing the unit cell volumes of the fourfold and sixfold coordinated phases versus pressure. The red squares and triangles represent the fourfold and sixfold coordinated phases (respectively) from the first cycle; blue squares and triangles represent the same for the second cycle. The solid arrows indicate direction of pressure change, and the dotted boxes indicate the mixed phase regions for the two cycles; the cycles overlap within experimental error. On the right is the shape change that a macroscopic wurtzite particle would undergo if the proposed mechanism were implemented.

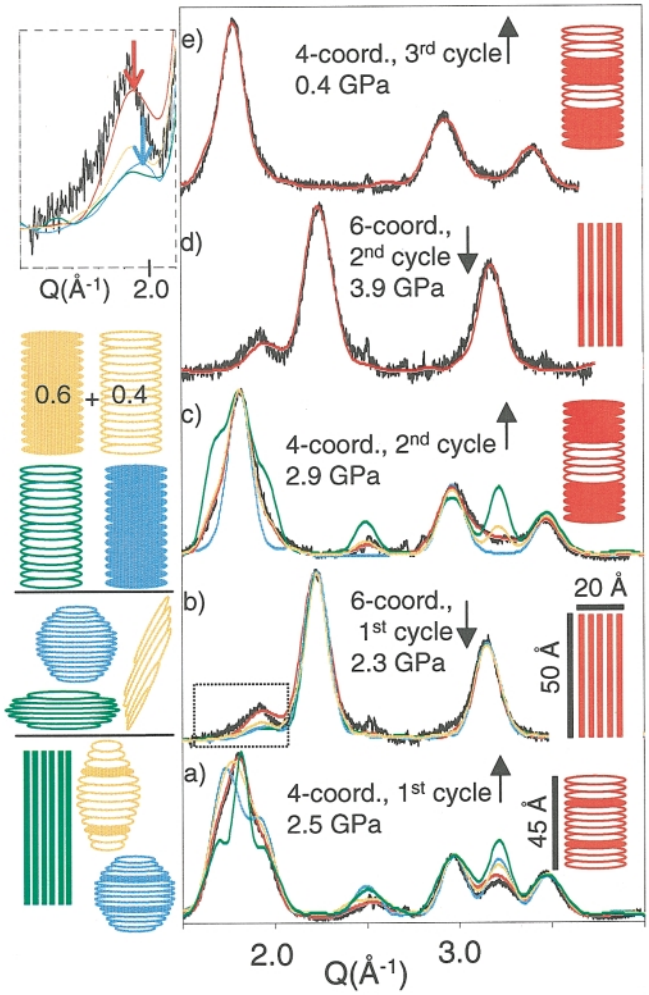

FIG. 2 (color). Sequence of shape changes found by comparing simulated patterns to the background subtracted experimental data (black). Shapes inside the figure boundary (in red) indicate the best fits. Layers indicate close-packed planes. Shaded planes indicate zinc-blende (*ABC*) stacking and white wurtzite (*ABA*) stacking. Blue, yellow, and green indicate shapes or stacking sequences that did not fit (shapes outside the figure boundary). (a) and (b) show the effects of different shapes on the fourfold and sixfold coordinated patterns, while (c) illustrates the effects of different types of stacking. All patterns shown are for particles with ~1800 atoms (same as a 45 Å sphere). The graph at the top left is a magnification of the boxed area in (b).

intensities must be considered in the analysis. Therefore, a diffraction simulation program was developed which allowed a detailed comparison of the observed patterns to simulated ones corresponding to specific structural models of the nanocrystals. The method is similar to that presented in previous papers on nanocrystal XRD [15]. The simulation was performed by generating a particle with the specified lattice structure, shape, and number of atoms, then generating the powder diffraction pattern using a discrete form of the Debye equation for powder diffraction [16,17]. The most important parameters in a fit are the shape of the nanocrystals, and, for the fourfold coordinated phase, arrangement of the close-packed planes in a hexagonal and/or cubic sequence (wurtzite and/or zinc blende, respectively) [18].

Figure 2 shows the strong sensitivity of the diffraction patterns towards structural parameters, as well as the best fits (red) throughout the cycles [19]. The nanocrystals start off as wurtzite with an average of two stacking faults per crystallite and a shape corresponding to either a cylinder with an aspect ratio of 1.2 (15 planes total) or an ellipse with an aspect ratio of 1.4 [here the unique axis of the hexagonal structure corresponds to the long axis of the particle; Fig. 2(a), red]. Under pressure they convert to a slab-shaped rock-salt structure [50 × 40 × 20 Å; Fig. 2(b), red], with one set of (111) planes parallel to the long axis; for this crystal structure, stacking faults are not a physical possibility. Here the high intensity of the (111) peak in the experimental pattern places severe constraints on the shape. In the slab shape, the (111) layers are oriented parallel to the large square face of the rectangle; the large number of contributing atoms increases the diffraction intensity for this reflection [red arrow, Fig. 2, magnification of (b)]. In contrast, the sphere and oblate sphere shapes [Fig. 2(b), blue, green] both have many small (111) layers, which causes the (111) peaks in their

diffraction patterns to have a lower relative intensity [blue arrow, Fig. 2, magnification of (b)].

After the particles transform back to a fourfold coordinated structure, they are more elongated than the pretransformed particles [Fig. 2(c)]; the shape is either a cylinder with an aspect ratio of 1.4 or an ellipse with an aspect ratio of 1.75. Remarkably, the retransformed particles contain stacking faults; the fit corresponds to a particle with three 5–6 layer domains, two zinc-blende domains separated by one wurtzite. Figure 2(c) also compares this pattern to those of pure zinc blende, pure wurtzite, and a 2:1 average of these two; from these it is clear that the experimental pattern is well represented only if both types of stacking are contained within one particle. Since stacking faults cannot exist in the parent rock-salt phase, the transition mechanism must account for their generation.

The shape changes which were observed during the first pressure cycle were reproducible. Figures 2(d) and 2(e) show the subsequent patterns fitted by the same sizes and shapes as the analogous patterns from the previous cycle (Figs. 2(b) and 2(c), respectively). The difference is in the planar disorder of the retransformed sample [Fig. 2(e)]; while the ratio of zinc blende to wurtzite stacking is still 2:1, the domain sizes are now three to four layers, instead of five to six.

The precise sequence of events during the phase transition cannot be specified completely by the above observations, but any proposed sequence must be consistent with them. For example, these observations preclude one pathway for this phase transition previously suggested by us [6], and also one proposed by Gupta and co-workers for bulk wurtzite CdS [20]. The former was a collapse along the unique axis of the particle, and the latter was a sliding-plane mechanism where the close-packed planes slide in alternate directions along the unique axis of wurtzite. Both of these mechanisms convert an elongated wurtzite nanocrystal to an oblate sphere in the rock-salt phase, a shape that clearly does not fit the data [Fig. 2(b), green]. In addition, neither mechanism is compatible with the stacking disorder in the initial and retransformed fourfold coordinated phases.

One mechanism that results in a shape change similar to the one seen in the data, and which is also consistent with the creation and destruction of stacking disorder, is shown in Fig. 3. It begins with the sliding of planes of atoms in the fourfold coordinated phase, in a manner similar to a martensitic phase transition. The motion transforms zinc blende or wurtzite to rock salt by converting (111) or (001) planes in the fourfold coordinated phase to (111) planes in the sixfold coordinated phase. The planes that slide in zinc blende are outlined by numbered dotted boxes in Fig. 3(a). If the stacking in zinc blende is denoted by *aAbBcC*, where a lowercase letter means a white atom and an uppercase means a gray one, then this is converted to *aBcAbC* in the rock-salt phase. This can be accomplished by many different sequences of planar shifts. One possibility is to fix layers 1 and 4, then shift 2 and 3 in opposite directions, as shown by the gray arrows in Fig. 3(a) (*aAbBcC* → *aBcAbC* directly) [21]. The result of successive planar shifting is shown in Fig. 3(b). To reach the final rock-salt structure [Fig. 3(c)], the atoms have to settle into the planes shown by the lines in Fig. 3(b) and then undergo a contraction and expansion along orthogonal directions. The macroscopic shape change that occurs if a wurtzite particle is converted to rock salt via this mechanism is shown in Fig. 1. Diffraction from this shape [Fig. 2(b), yellow] is not the same as that from the best fit; while it does contain large (111) planes, they are not as large as those in a particle with a perfect slab geometry. We emphasize that we are describing the types of motions consistent with the observed structural changes, but the precise sequence of events is not determined; for that, a detailed theoretical investigation is required [22].

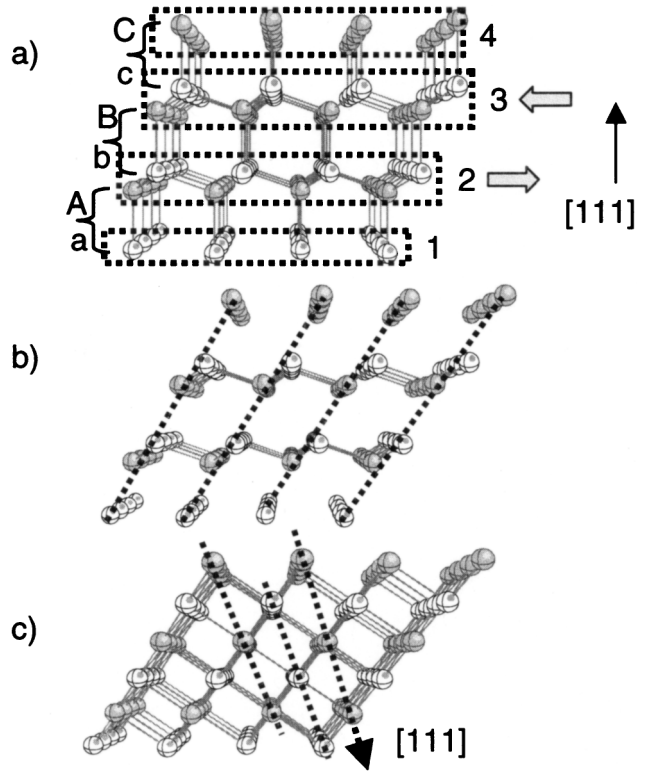

FIG. 3. Proposed mechanism of sliding planes. (a) Zinc-blende structure. Brackets indicate (111) planes, dashed boxes indicate planes of atoms that slide together, and gray arrows indicate the directions of slides. (b) The structure of (a) after sliding successive planes. (c) Rock-salt structure; the dotted lines indicate (111) planes. All structures are presented with the same orientation.

This mechanism of planar shifts has important consequences for the kinetics of the phase transition. It may mean that the activation energy for this mechanism should scale with the area of a plane, rather than the volume of a particle. This is markedly different from the simple volume scaling of the barrier to magnetization reversal in the Néel model [3]. This mechanism also explains the presence of planar disorder in the retransformed phase; stacking faults can be generated if successive planes shift in

different (energetically equivalent) directions, so that ultimately entropic rather than energetic factors determine the population of the planes after many successive cycles.

In summary, high-pressure XRD patterns of CdSe nanocrystals show that the original and retransformed fourfold coordinated structures are not the same; simulations to fit the data show that the retransformed particles are elongated, mixed-phase structures. Furthermore, the sixfold coordinated phase is best fit to a slab shape. Based on these observations, we propose a mechanism of planar shifts where the activation energy should scale with the area of a plane rather than the total volume of the particle. Recent synthetic advances have allowed us to control the morphology of CdSe nanocrystals, creating "quantum rods" that are highly elongated along the unique axis of wurtzite [23]. Based on the proposed mechanism, we predict that, for a fixed short axis size (fixed planar area), the activation energy will not vary with the length of the long axis.

This work was supported by the Director, Office of Energy Research, Office of Basic Energy Sciences, Division of Materials Sciences, of the U.S. Department of Energy under Contract No. DE-AC03-76SF00099. X-ray diffraction experiments were performed using the facilities of the University of California-LLNL PRT at the Stanford Synchrotron Radiation Laboratory, which is operated by the DOE, Division of Chemical Sciences.

*Current address: Exxon Research and Engineering Company, Corporate Research Science Laboratory, Route 22 East, Annandale, NJ 08801

[1] M. L. Cohen, Science **234**, 549 (1986); V. Ozolins, C. Wolverton, and A. Zunger, Phys. Rev. B **57**, 6427 (1998).

[2] K. Mizushima, S. Yip, and E. Kaxiras, Phys. Rev. B **50**, 14 952 (1994); L. E. Brus, J. A. W. Harkless, and F. H. Stillinger, J. Am. Chem. Soc. **118**, 4834 (1996).

[3] L. Néel, Ann. Geophys. **5**, 99 (1949); W. F. Brown, Phys. Rev. **130**, 1677 (1963); W. Wernsdorfer *et al.,* Phys. Rev. Lett. **78**, 1791 (1997).

[4] G. Bertotti, *Hysteresis in Magnetism* (Academic Press, San Diego, 1998).

[5] M. R. Silvestri and J. Schroeder, J. Phys. Condens. Matter **7**, 8519 (1995); A. A. Gribb and J. F. Banfield, Am. Mineral. **82**, 717 (1997); T. Nanba *et al.,* J. Phys. Soc. Jpn. **66**, 1526 (1997).

[6] S. H. Tolbert and A. P. Alivisatos, Science **265**, 373 (1994); S. H. Tolbert and A. P. Alivisatos, J. Chem. Phys. **102**, 4642 (1995).

[7] C.-C. Chen *et al.,* Science **276**, 398 (1997).

[8] Note that this single domain behavior is observed in discrete nanocrystals that are isolated from each other. Very different kinetics is seen in aggregated nanoparticle systems, which have a profusion of grain boundaries and interacting domains. H. Gleiter, Nanostruct. Mater. **1**, 1 (1992); J. Z. Jiang *et al.,* Europhys. Lett. **44**, 620 (1998).

[9] S. H. Tolbert *et al.,* Phys. Rev. Lett. **76**, 4384 (1996).

[10] C. B. Murray, D. J. Norris, and M. G. Bawendi, J. Am. Chem. Soc. **115**, 8706 (1993); J. E. B. Katari, V. L. Colvin, and A. P. Alivisatos, J. Phys. Chem. **98**, 4109 (1994); X. G. Peng, J. Wickham, and A. P. Alivisatos, J. Am. Chem. Soc. **120**, 5343 (1998).

[11] J. D. Barnett, S. Block, and G. J. Piermarini, Rev. Sci. Instrum. **44**, 1 (1973).

[12] A. L. Edwards and H. G. Drickamer, Phys. Rev. **122**, 1149 (1961); A. Jayaraman, W. J. Klement, and G. C. Kennedy, Phys. Rev. **130**, 2277 (1963); A. Onodera, Rev. Phys. Chem. Jpn. **39**, 65 (1969).

[13] S. H. Tolbert and A. P. Alivisatos, Annu. Rev. Phys. Chem. **46**, 595 (1995).

[14] R. E. Hanneman, M. D. Banus, and H. C. Gatos, J. Phys. Chem. Solids **25**, 293 (1964); U. D. Venkateswaran, L. J. Cui, and B. A. Weinstein, Phys. Rev. B **45**, 9237 (1992).

[15] M. G. Bawendi *et al.,* J. Chem. Phys. **91**, 7282 (1989); C. B. Murray, D. J. Norris, and M. G. Bawendi, J. Am. Chem. Soc. **115**, 8706 (1993); C. L. Cleveland *et al.,* Phys. Rev. Lett. **79**, 1873 (1997).

[16] B. D. Hall and R. Monot, Comput. Phys. **5**, 414 (1991).

[17] Multiplying the Debye formula by a decaying exponential containing the angle-dependent Debye-Waller factor can simulate the effect of temperature. This factor alone allows the relative intensity of patterns taken on a conventional diffractometer to be simulated, but geometric considerations cause the intensity of patterns collected at the synchrotron to drop off faster. Therefore, a cubic function was generated which forced an intensity fit of the most pronounced peaks in the simulated pattern to the same peaks in the experimental pattern, after the normalization of the same peak in both patterns.

[18] Bond length distortions at the surface have no observable effect on the simulated patterns, while systematic distortions throughout the volume of the particle (such as a radial contraction) cause the relative peak positions to change, so neither effect was included in the final analysis.

[19] Patterns in Fig. 2 were taken at low pressures (1–4 GPa) to avoid a slight, reversible line broadening (due to nonhydrostatic pressure gradients) that occurs at higher pressures (9–11 GPa).

[20] M. D. Knudson, Y. M. Gupta, and A. B. Kunz, Phys. Rev. B **59**, 11 704 (1999).

[21] The same end result can be reached if layers shift successively in the sequence *aAbBcC* to *aBcCaA* to *aBcAbB* to *aBcAbC* [resulting in the shape shown in Fig. 3(b)]. To convert wurtzite, a preliminary shift is required (not shown), which locally converts the shifting layers to zinc-blende-type stacking (for example, *aAbBaA* to *bBcCaA*). Subsequent planar movement is the same as that required for zinc blende.

[22] R. Martonak, C. Molteni, and M. Parrinello (private communication).

[23] X. Peng *et al.,* Nature (London) (to be published).